New Terpyridine-based Ruthenium Complexes for Dye Sensitized Solar Cells Applications

Ganesh Koyyada, C.H. Pavan Kumar, Paolo Salvatori, Gabriele Marotta, Maria Grazia Lobello, Olivia Bizzarri, Filippo De Angelis, Chandrasekharam Malapaka

PII: S0020-1693(15)00595-2
DOI: http://dx.doi.org/10.1016/j.ica.2015.11.031
Reference: ICA 16789

To appear in: *Inorganica Chimica Acta*

Received Date: 28 July 2015
Revised Date: 19 October 2015
Accepted Date: 28 November 2015

Please cite this article as: G. Koyyada, C.H. Pavan Kumar, P. Salvatori, G. Marotta, M.G. Lobello, O. Bizzarri, F. De Angelis, C. Malapaka, New Terpyridine-based Ruthenium Complexes for Dye Sensitized Solar Cells Applications, *Inorganica Chimica Acta* (2015), doi: http://dx.doi.org/10.1016/j.ica.2015.11.031

New Terpyridine-based Ruthenium Complexes for Dye Sensitized Solar Cells Applications

Ganesh Koyyada,[a,b] Pavan Kumar CH,[a,b] Paolo Salvatori,[c,d] Gabriele Marotta,[c,e] Maria Grazia Lobello,[c] Olivia Bizzarri,[c] Filippo De Angelis*,[c] Chandrasekharam Malapaka*.[a,b]

[a]Inorganic and Physical Chemistry Division, CSIR-Indian Institute of Chemical Technology, Uppal Road, Tarnaka, Hyderabad 500607, India.

[b]Academy of Scientific and Innovative Research, CSIR-IICT, India.

[c]Computational Laboratory for Hybrid and Organic Photovoltaics, Istituto CNR di Scienze e Tecnologie Molecolari, via Elce di Sotto 8, 06123, Perugia, Italy.

[d]D3-Computation, Istituto Italiano di Tecnologia, Via Morego 30, I-16163 Genova, Italy.

[e]Dipartimento di Chimica, Biologia e Biotecnologie, Universitàdegli Studi di Perugia, via Elce di Sotto 8, I-06123 Perugia, Perugia, Italy.

E-mail: Chandra@iict.res.in Phone Fax : +00914027193186.

Keywords: Dye sensitized solar cell (DSSC), Thiocyanate free, Single Thiocyanate, Efficiency, DFT/TDDFT

Abstract

Three new Terpyridine-based ruthenium complexes, named as **MC124**, **MC125** and **MC127**, were synthesized and employed as sensitizers in Dye Sensitized Solar Cells. The **MC** dyes were characterized with experimental techniques followed by theoretical calculations. The promising optical properties with higher molar extinction coefficients compared to **N749** prototypical dye, and suitable positioning of energy levels prompted us to employ these dyes in working devices. When used in conjunction with liquid I^-/I_3^- redox electrolyte, the **MC** dyes have shown modest performances, with a maximum PCE of 2.3% reached with **MC124** in combination of CDCA used as co-adsorbent.

1. Introduction

Dye-sensitized solar cells (DSSCs) are considered to be one of the alternative next generation photovoltaic devices due to their ease of fabrication, low materials cost and attractive unique features.[1] Typical DSSCs is based on a photoelectrode with mesoporous anatase TiO_2 layer,[2,3] usually composed by a network of nanoparticles (~ 20/30 nm diameter), sensitized with dye molecules and interpenetrated by a liquid electrolyte (usually I^-/I_3^- redox couple in a volatile organic solvent). The device architecture is completed by a counter-electrode. After the photoexcitation of the chemisorbed dye, charge separation occurs at the dye/TiO_2 interface with electron injection into the semiconductor conduction band (CB). The injected electrons flow across the mesoporous structure of TiO_2 layer and through the external circuit is collected at the counter electrode. The oxidized dye molecules are regenerated by the redox mediator in the telectrolyte solution and finally, the circuit is closed by the electrolyte regeneration at the counter-electrode.

In the past decade, number of modifications have been attempted on sensitizers, TiO_2 photo electrodes, counter electrodes and electrolyte composition in order to improve the overall performance of DSSCs.[4-8] Sensitizers are the key element to the success of this technology as the power conversion efficiency of the device is known to be greatly influenced by light harvesting and electron injection properties of the sensitizer.. A large variety of sensitizers have been tested for DSSCs including organic dyes,[9-13] zinc porphyrin[14-16] and Ru(II)-based ~~organometallic~~ sensitizers.[17-19, 55]

Although the high power conversion efficiencies (PCE) have been reached with organic dyes (approaching 10%)[20,21] and with porphyrin sensitizers in combination with Cobalt based redox couple (13%),[22-24] the Ru(II)polypyridyl ~~organometallic~~ sensitizers are continued to be deeply

investigated. Apart from molecular sensitizers, recently perovskite hybrid absorbers ($MAPbI_3$, where MA = methylammonium or other derivatives) have shown 19% efficiency in solid state devices.[25-27] However, health hazards due to lead perovskites are a critical issue that may undermine its future employment and hence scientists are encouraged to continuously stay on the track of traditional DSSCs.

One of the prototypical terpyridyl ruthenium (II) sensitizer $[Bu_4N]_3[Ru(tctpy)(NCS)_3]$,was reported by Nazeeruddin and coworkers.[28] This sensitizer, also known as N749 or black dye, has shown an impressive efficiency of 10.4%. When used in combination with an organic cosensitizer, an improved certified record efficiency of 11.4% has been reported.[45] Though ruthenium (II) terpyridyl complexes show better photo response in longer wavelength region than those of bipyridyl complexes, the disadvantage generally lies with its low incident to photon conversion efficiency due to poor molar extinction coefficient and insufficient free energy for electron injection.[29] Extensive research has been pursued on functionalization of the N749 structure, with electron rich units, in order to increase light harvesting capacity and the charge transfer efficiency.[30-33] Other possible strategies employed to improve the efficacy in both the visible and near-IR regions, are the tandem DSSCs [35–36] or the cosensitization.[37–42]

Concerning the stability in working devices, the **N749** dyes have shown similar performances compared to other Ru-bipyridyl dyes.[43] The presence of sulphur group in thiocyanate based ruthenium (II) sensitizers makes intimate contact with the iodide redox couple of the electrolyte that helps in the regeneration of dye.[44] Despite of these advantages, thiocyanates are weakly coordinating to the ruthenium (II) center and can be substituted by electrolyte additives, such as tert-butyl pyridine, or solvent molecules, under Stressing thermal and light soaking conditions.[45-47]

Being already engaged in synthesis of various ruthenium and metal free sensitizers,[48-55] we have designed a new class of ruthenium (II) sensitizers by partially or fully replacing the thiocyanate groups in black dye with bipyridine and terpyridine ligands as shown in **Figure1**, which is presumed to improve the absorption properties in the longer wavelength region. The bipyridines were functionalized with carbazole and fluorene as ancillary groups because of their hole transport capability, electron-richness and elongated conjugation. Furthermore alkyl chains introduced on the fluorene, carbazole and terpyridine moieties are expected to inhibit the dye aggregation and interfacial electron recombination processes. Here taking advantage of the support from theoretical calculations, we demonstrate the synthesis, the characterization and the photovoltaic performance of these three new terpyridine-based ruthenium complexes suitable for applications in DSSCs.

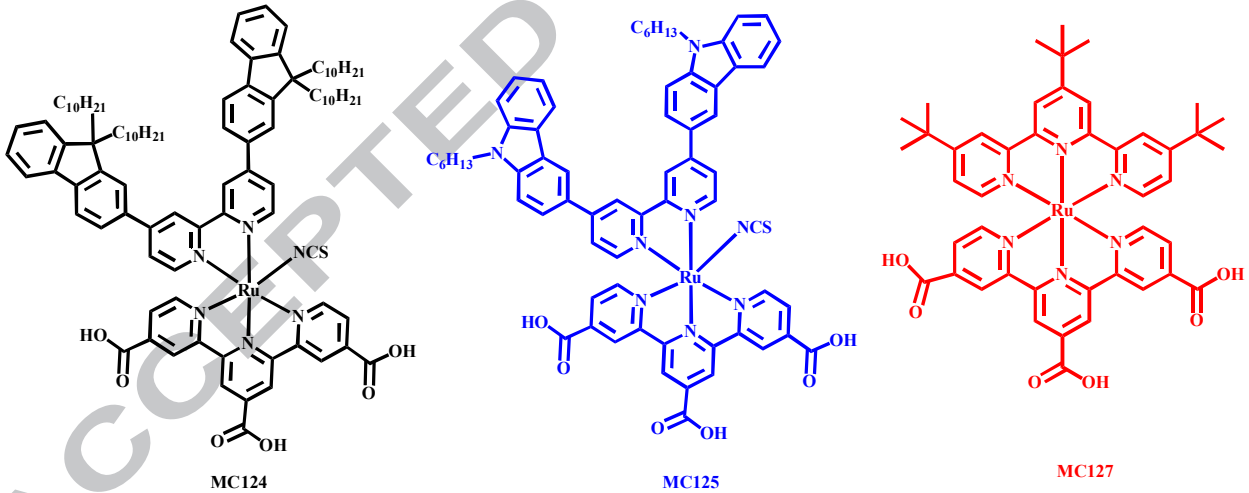

Figure 1. Structures of **MC124**, **MC125** and **MC127**

2. Experimental details

2.1 Materials and instrumentation

The starting materials were purchased from Sigma-Aldrich. The solvents were purified using standard procedures and purged with nitrogen before use. All other chemicals used in this work were analytical grade and were used without further purification, and all reactions were performed under argon atmosphere. Absorption spectra were recorded on a Shimadzu ultraviolet-visible light (UV-vis) spectrometer. Emission spectra were recorded on a J. Y. Horiba model fluorolog3 fluorescence spectrometer. The Differential Pulse Voltametry (DPV) curves were recorded using BAS100 electrochemical analyser where a three electrode cell is used in 0.1 M Bu_4NPF_6, N,N-dimethylformamide as solvent at a scan rate of 100 mVs^{-1}, Pt wire as a counter electrode , Ag/AgCl as reference electrode and calibrated with ferrocene.

2. 2 ***2-bromo-9,9-didecyl-9H-fluorene (1)*** (83%)**.** To an ice-cooled suspension of KOH (0.137 g, 2.459 mmol) in DMSO (10 mL), 2-bromo-9H-fluorene (0.200 g, 0.819 mmol) and 1-bromodecane (0.345 mL, 2.276 mmol) was added. The suspension was stirred at room temperature for 16 h under N_2. The mixture was cooled at room temperature and brine was added. The organic layer was extracted with ethylacetate and the combined organic extractions were dried over Na_2SO_4. After evaporation of solvent, the crude compound was purified over silica gel column and eluted using ethylacetate:hexane (1:9).

^{1}H NMR (300 MHz, $CDCl_3$, δ): 7.64-7.68 (m, 1H), 7.53-7.56 (m, 1H), 7.42-7.46 (m, 2H), 7.30-7.34 (m, 3H), 1.86-1.94 (m, 4H), 1.22-1.28 (m, 4H), 1.16-1.20 (m, 10H) 1.12-1.15 (m, 4H), 1.00-1.10 (m, 14H), 0.9 (t, 6H); ^{13}C NMR (300MHz, $CDCl_3$, δ): 14.11, 22.65, 23.65, 29.22, 29.52, 29.93, 31.85, 40.24, 55.34, 119.70, 120.92, 120.98, 122.83, 126.08, 128.87, 127.41, 129.82, 130.98, 140.09, 150.26, 152.92. ESI-MS:m/z $[M]^+$: 526.

2.3 ***2-(9,9-didecyl-9H-fluoren-7-yl)-4,4,5,5-tetramethyl-1,3,2-dioxaborolane (2)*** (82%).A solution of compound (**1)** (0.500 g, 0.952 mmol), bis(pinacolato)diboron (0.265 g, 1.047 mmol), were dissolved in dry dimethoxy ethane (8 mL) and KOAc (0.227 g, 2.856 mmol) was added. The mixture was stirred for 15 min under an argon atmosphere at room temperature. Then $Pd(dppf)_2Cl_2$ (0.041 g, 0.057 mmol) catalyst was added and the reaction mixture was stirred

overnight at 80 ^{0}C. After being cooled to room temperature, the mixture was poured into water (20 mL) and the organic layer was separated. The aqueous layer was extracted with dichloromethane (3 X 20 mL) and the combined organic layers were dried over anhydrous Na_2SO_4. The organic solvent was evaporated under reduced pressure and the crude product was pre-adsorbed onto silica gel and chromatographed (8:2 *n*-hexane/ethyl acetate) to give yellow viscous liquid **2**

^{1}H NMR (300 MHz, $CDCl_3$, δ): 7.78-7.82 (m, 1H), 7.74-7.76 (m, 1H), 7.68-7.73 (m, 2H), 7.30-7.36 (m, 3H), 1.92-2.02 (m, 4H), 1.39 (s, 12H), 1.20-1.32 (m, 8H), 1.10-1.20 (m, 12H) 0.98-1.08 (m, 12H), 0.88 (t, 6H); ^{13}C NMR (300MHz, $CDCl_3$, δ): 14.13, 22.69, 23.71, 24.96, 29.29, 29.57, 30.05, 31.88, 40.25, 55.07, 83.69, 118.95, 120.09, 122.94, 126.66, 127.48, 128.82, 133.70, 140.92, 144.12, 149.88, 151.30. ESI-MS:m/z $[M]^+$: 572.

2.4 ***4-(9,9-didecyl-9H-fluoren-2-yl)-2-(4-(9,9-didecyl-9H-fluoren-7-yl)pyridin-2-yl)pyridine (L1)*** (76 %)**.** A 50 mL of Schlenk tube was charged with aryl 4,4'-dibromobipyridine (0.500 g, 1.592 mmol) compound **(2)** (1.912 g, 3.343 mmol), $Pd(PPh_3)$ (0.115 g, 0.1 mmol). Dimethoxy ethane (8 mL), 2 M aqueous sodium carbonate (2 mL) were added and the tube was purged with argon gas with 5 evacuate /refill cycles. The tube was sealed and heated at 90 ^{0}C for 18 h. Upon cooling to ambient temperature, the organics were extracted into dichloromethane (3 × 30 mL) from 30 mL water. The combined organics were washed with water (1 × 30 mL) and brine (1 × 30 mL), dried over Na_2SO_4, filtered and the solvent was removed under reduced pressure. The crude compound was purified by silica gel column chromatography using hexane/ethyl acetate (9:1) to give light yellow powder.

^{1}H NMR (300 MHz, $CDCl_3$, δ): 8.80-8.04 (m, 4H), 7.74-7.88 (m, 8H), 7.64-7.68 (m, 2H), 7.32-7.40 (m, 6H), 2.00-2.32 (m, 8H), 1.24-1.28 (m, 8H), 1.12-1.20 (m, 14H), 0.9 (t, 12H); ^{13}C NMR

(300MHz, $CDCl_3$, δ): 14.08, 22.63, 23.77, 29.69, 30.43, 31.49, 31.62, 31.92, 33.82, 40.35, 55.34, 114.05, 121.33, 121.82, 122.92, 123.45, 126.18, 126.85, 127.52, 136.88, 139.23, 140.33, 142.29, 149.53, 149.98, 151.13, 151.66, 156.73.ESI-MS:m/z $[M+H]^+$:1046

2.5 ***3-bromo-9-hexyl-9H-carbazole (3)*** (82%)**.** The synthesis procedure resembles that of compound (**1**) with 1-bromohexane (0.093 mL, 0.666 mmol) instead of 1-bomodecane in DMF solvent. Viscous liquid (**3**) was obtained. ^{1}H NMR (300 MHz, $CDCl_3$, δ): 8.18 (d, 1H), 8.00-8.04 (d, 1H), 7.49-7.54 (m, 1H), 7.44-7.47 (m, 1H), 7.36-7.40 (m, 1H), 7.20-7.25 (m, 1H), 7.19-7.22 (m,1H), 4.21-4.26 (t, 2H), 1.77-1.87 (m, 2H), 1.23-1.36 (m, 6H), 0.9 (t, 3H); ^{13}C NMR (300MHz, $CDCl_3$, δ): 13.97, 22.48, 26.85, 28.79, 31.48, 43.05, 108.83, 110.01, 119.06, 120.4, 121.68, 122.93, 124.93, 124.42, 126.22, 128.08, 128.85, 138.92. ESI-MS:m/z $[M]^+$: 330.

2.6 ***9-hexyl-3-(4,4,5,5-tetramethyl-1,3,2-dioxaborolan-2-yl)-9H-carbazole (4)*** (80%). The synthesis method resembles that of compound (**2**). Colorless liquid (**4**) was obtained. ^{1}H NMR (300 MHz, $CDCl_3$, δ): 8.60 (s, 1H), 8.06 (d, 1H), 7.86 (d, 1H), 7.42-7.44 (m, 1H), 7.38-7.40 (m, 2H), 7.20-7.23 (m, 1H), 4.22-4.36 (t, 2H), 1.82-1.86 (qt, 2H), 1.40 (s, 12H), 1.22-1.38 (m, 6H), 0.9 (t, 3H); ^{13}C NMR (300MHz, $CDCl_3$, δ): 13.93, 22.45, 24.88, 26.86, 28.82, 31.50, 43.00, 83.47, 108.01, 108.65, 119.11, 120.47, 122.54, 123.06, 125.51, 127.69, 132.09, 140.54, 142.54. ESI-MS:m/z $[M+H]^+$:338.

2.7 ***9-hexyl-3-(2-(4-(9-hexyl-9H-carbazol-6-yl)pyridin-2-yl)pyridin-4-yl)-9H-carbazole (L2)*** (73%). The synthesis method resembles that of compound (**L1**). White powder of (**L2**) was obtained.^{1}H NMR (300 MHz, $CDCl_3$, δ): 8.84-8.86 (m, 2H), 8.78-8.82 (m, 2H), 8.58-8.60 (m, 2H), 8.20-8.22 (m, 2H), 7.96-7.98 (m, 2H), 7.72-7.76 (m, 2H), 7.50-7.56 (m, 4H), 7.44-7.48 (m, 2H), 7.28-7.32 (m, 2H), 4.36-4.40 (t, 4H), 1.88-1.96 (qt, 4H), 1.56-1.64 (m, 4H), 1.40-1.48 (m, 4H), 1.28-1.36 (m, 4H),0.9 (t, 6H); ^{13}C NMR (300MHz, $CDCl_3$, δ): 13.99, 22.51, 26.94, 28.92,

31.54, 43.21, 108.92, 109.08, 119.05, 119.18, 119.22, 120.59, 121.54, 122.80, 123.41, 124.87, 126.03, 128.80, 140.89, 140.94, 149.50, 150.17, 156.71.ESI-MS:m/z $[M+H]^+$:656.

2.8 ***4,4',4''-trimethoxycarbonyl-2,2':6',2''-terpyridine (5) and trimethyl [2,2':6',2''-terpyridine]-4,4',4''-tricarboxylate Ruthenium(III) trichloro*** **(6)** were reported in our previous literature (RSC Adv., 2013, 3, 26035–26046)

2.9 ***General procedure for the synthesis of ruthenium complex (MC124*** *and* ***MC125)***

A solution of ligand **L** (0.272 mmol) and ruthenium trichloro complex (0.227 mmol) dissolved in dry DMF (100 mL) was heated and refluxed for 4 h under nitrogen atmosphere in the dark. After completion of 4 h, the mixture was cooled to 80^0C. To the resulting dark green solution was added aqueous solution of NH_4NCS (0.573 g in 2 mL of water) and the reaction mixture was further refluxed for 2 h. The progress of the reaction was monitored by UV-Vis spectroscopy. After 2 h, the reaction mixture was cooled to room temperature and triethylamine was added followed by water (2 ml+2 mL). The mixture was further refluxed for 48 h. Then the reaction mixture was cooled to room temperature and the solvent was removed under reduced pressure and water (200 mL) was added to get precipitate. The purple solid was filtered off and washed with distilled water, ether and dried under vacuum. The crude compound was dissolved in methanol and Terrabutylammonium hydroxide (TBA), further purified on sephadex LH-20 with methanol as eluent. The main band was collected and concentrated to give

MC124 (63%)**.** ^{1}H NMR (300 MHz, $CDCl_3$+CD_3OD, δ): 8.96-9.24 (m, 2H), 8.76-8.84 (m, 2H), 8.68-8.72 (m, 2H), 7.96-8.48 (m, 2H), 7.84-7.92 (m, 6H), 7.72-7.82 (m, 4H), 7.52-7.64 (m, 2H), 7.44-7.48 (m, 2H), 7.32-7.40 (m, 6H) 1.96-2.20 (m, 8H), 1.14-1.36 (m, 64H), 0.9 (t, 12H); FT-IR (KBr) (cm^{-1}): 3064, 2924, 2852, 2092, 1604, 1450, 1364, 1235, 1019. Anal. cal.:

$C_{96}H_{115}N_5O_6RuS$. C: 73.53, H: 7.39, N: 4.47, S: 2.04 found: C: 73.50, H: 7.32, N: 4.41, S: 2.01%.

MC125 **(**60%**).** ^{1}H NMR (300 MHz, $CDCl_3$+CD_3OD, δ): 8.76-8.84 (m, 4H), 8.56-8.64 (m, 2H), 8.20-8.28 (m, 3H), 7.92-8.00 (m,3H), 7.76-7.82 (m, 3H), 7.44-7.60 (m, 8H), 7.21-7.32 (m, 4H), 7.04-7.08 (m, 1H), 4.36 (t, 4H), 3.56-3.76 (m, 4H), 1.88-2.08 (m, 4H), 1.52-1.64 (m, 2H), 1.24-1.32 (m, 4H), 0.9 (t, 8H); FT-IR (KBr) (cm^{-1}): 3416, 2921, 2852, 2097, 1594, 1466, 1365, 1237, 1156.Anal. cal.: $C_{66}H_{57}N_7O_6RuS$. C: 67.33, H: 4.88, N: 8.33, S: 2.72 found: C: 67.30, H: 4.82, N: 8.29, S: 2.69%.

MC127 (58%).The synthesis method resembles that of **MC124** and **MC125**, except that NH_4NCS was not added.

^{1}H-NMR (300 MHz, $CDCl_3$, □): 9.23(s, 2H), 8.96 (s, 2H), 8.75 (s, 2H), 8.44 (s, 2H), 7.57-7.56 (d, 2H), 7.17(m, 2H), 712 (m, 2H), 7.09 (m, 2H), 1.72 (s, 9H), 1,27 (s, 18H).FT-IR (KBr) (cm^{-1}): 785.96, 915.56, 1033.08, 1242.02, 1354.83, 1400.58, 1541.55,1610.93, 2957.57, 3399.82.ESI-MS:m/z $[M+H]^+$:869; Anal Calcd for $C_{45}H_{46}N_6O_6Ru$, C, 62.17; H, 5.34; N, 9.64; found C, 61.87; H, 5.39; N, 9.47.

2.10 Device fabrication

Fluorine doped Tin Oxide (FTO) coated glass (Nippon Sheet Glass,4 mm, 10 Ω/cm^2), ..was cleaned by sonication in an aqueous solution of Deaconex 21 (0.2 % wt) followed by 30 min at 500 ^oC. To form a dense blocking layer, the substrates were treated in 40 mM aqueous $TiCl_4$ solution (70 °C, 30 min) and rinsed with deionized water. A 12 μm layer of transparent paste (18 NR-T, Dyesol) was spread on the FTO glass by screen printing. Next a 4μm scattering layer was deposited over the transparent layer by using the same screen printing process. Different film thicknesses were obtained by repeating the screen printing step several times. In this case the

films were dried at 125 °C for 5 min between each print. The TiO_2-coated electrodes (active area 0.28 cm^2) were gradually heated under air flow at 325 °C for 5 min, at 375 °C for 5 min, at 450 °C for 15 min, and 500 °C for 15 min. A post treatment with $TiCl_4$ was applied using 40 mM aqueous $TiCl_4$ solution at 70 °C for 30 min. The area of the deposited films was 0.28 cm^2. After reheating the photoanodes to 500°C for 30 min, they were cooled down to about 80 °C and then immersed into the dye solutions (0.3 mM and when required 0.6 mM 3a, 7a-dihydroxy-5b-cholic acid (CDCA) added) containing 10% DMF in acetonitrile and tert-butyl alcohol (volume ratio 1:1) for 20 h. Following the immersion procedure the sensitized electrodes were shortly rinsed with acetonitrile and dried in air. Counter electrodes were fabricated by drop casting a H_2PtCl_6 solution (5 mM in isopropanol) onto TEC7 FTO-coated Glass (Solaronix 2.2mm, 7 Ω/cm^2) and fired in air at 400 °C for 5 min. These procedures were replicated two times. Cells were assembled using a 25 μm thick Surlyn thermoplastic resin (DuPont) and sealed by heating. The Z960 liquid electrolyte (1.0 M 1,3-dimethylimidazolium iodide (DMII), 50 mM LiI, 30 mM I_2, 0.5 M *ter*-butylpyridine, and 0.1 M guanidiniumthiocyanate (GNCS) in a mixture of acetonitrile/valeronitrile (v/v, 85/15) was introduced via two holes made previously on the counter electrode. The holes were sealed with Surlyn and a glass cover slip.

2.11 Photovoltaic characterization

The solar cells were measured using a 450 W xenon light source (Oriel) with an irradiance of 100 mW/cm^2 at the surface of the devices. A Schott K113 Tempax filter (PräzisionsGlas & Optik GmbH) was used to reduce the spectral mismatch between AM1.5G and the simulated illumination to approximately 4% between 350-750 nm. Different light intensities were obtained using wavelength neutral wire mesh attenuators (RHB) and calibrated with a Si-photodiode equipped with an IR-cutoff filter (KG3, Schott). Current-Voltage characteristics of the cells were

obtained by applying an external voltage bias (from V_{oc} to 0 V) to the cell while measuring the current response with a digital source meter (Keithley 2400). The voltage step and equilibration times were 10 mV and 80 ms, respectively. The cells were covered with a thin mask (0.16 mm^2) to reduce scattered light. Incident-photon-to-collected-electron efficiency (IPCE) spectra were measured using a home built system composed of a 300 W xenon lamp (ILC Technology), a Gemini-180 double monochromator with 1200 grooves/mm grating (JobinYvon Ltd) and a lock-in amplifier (SR830 DSP, Stanford Research Systems). The incident monochromatic light was chopped at a frequency of approximately 2 Hz and was superimposed onto a constant white light bias of 10 mW/cm^2 supplied by a LED array in order to provide a sufficient base conductivity of the mesoporous TiO_2 for charge collection.

2.12 Computational details

All the calculations have been performed by the Gaussian 09 program package.[56] We optimized the molecular structures using the B3LYP exchange–correlation functional[57] and a 3-21G* basis set[58] in vacuo. TDDFT calculations of the lowest singlet–singlet excitations were performed in DMF solution, on the optimized geometries using the B3LYP functional and a DGDZVP basis set.[59] The C-PCM[60,61] was employed for including the solvent effects in TDDFT calculations, as implemented in G09. To simulate the optical spectra, the 70 lowest spin-allowed singlet–singlet transitions were computed on the ground state geometry. Excitation energies and oscillator strengths were interpolated by a Gaussian convolution with a σ value of 0.14 eV, corresponding to an FWHM of ~0.35 eV.

3. Results and discussion

3.1 Synthesis

The synthetic route for **MC124**, **MC125** and **MC127** were shown in the Scheme 1. The commercially available starting materials 2-bromo-9H-fluorene and 3-bromo-9H-carbazole were subjected to alkylation followed by their conversion from bromo to boronic ester 2-(9,9-didecyl-9H-fluoren-2-yl)-4,4,5,5-tetramethyl-1,3,2-dioxaborolane (**2**) and 9-hexyl-3-(4,4,5,5-tetramethyl-1,3,2-dioxaborolan-2-yl)-9H-carbazole (**4**) respectively with good yields of 82% and 83% respectively. Intermediates **2** and **4** further subjected to coupling with dibromobipyridine under Suzuki conditions to afford 4,4'-bis(9,9-didecyl-9H-fluoren-2-yl)-2,2'-bipyridine (**L1)** and 9-hexyl-3-(2-(4-(9-hexyl-9H-carbazol-6-yl)pyridin-2-yl)pyridin-4-yl)-9H-carbazole (**L2)** respectively in yields of 76% and 73% respectively. The final step was performed by typical one pot synthesis using [$RuCl_3$(tetp)] (tercarbmethoxyterpyridine) with ancillary ligand L1/L2/L3(commercially available) at 150°C for 4h using DMF as solvent, then chlorine ligand was substituted by thiocyanate ligand, followed by ester hydrolysis using base catalyzed conditions to afford the Ru-complexes in good yields. Details on the synthetic procedure and complete characterization of the intermediates and the products were presented in the experimental part.

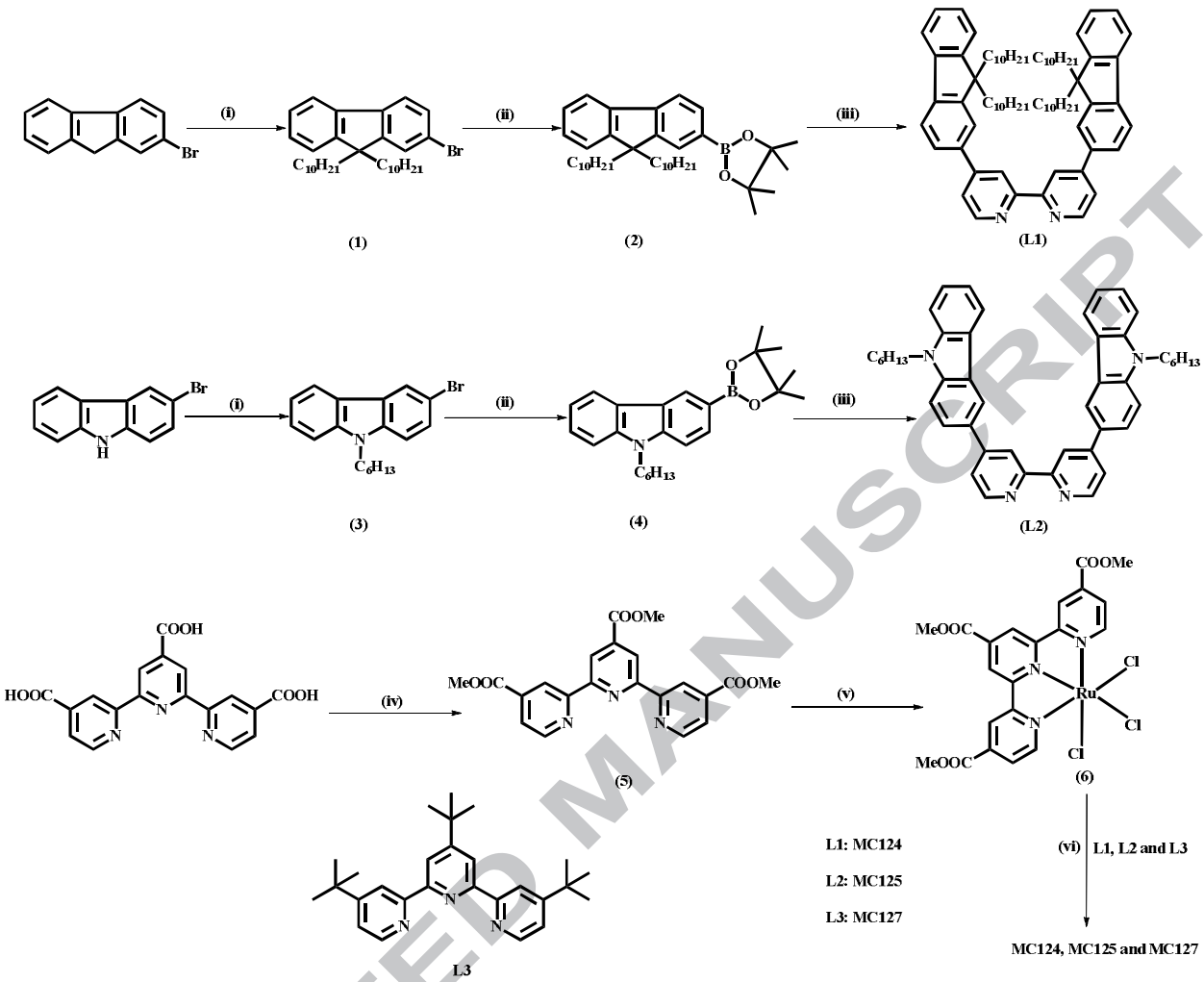

Scheme1. Synthesis of sensitizers **MC124**, **MC125** and **MC127**. Reagents and conditions: i) KOH, DMSO, 1-bromodecane, RT, 18 h; ii) $B_2(pin)_2$, $Pd(dppf)_2Cl_2$, KOAc, DME, 90 ^{0}C, 18 h; iii) $Pd(PPh_3)_4$, 2M Na_2CO_3, DME, 90 ^{0}C, 18 h; iv) MeOH, conc. H_2SO_4, reflux, 6 hours; v) $RuCl_3.3H_2O$, EtOH/$CHCl_3$, reflux under dark, 4 hours; vi) L1-L3, DMF reflux, 4 hours then NH_4NCS, reflux, 2 hours then TEA, water, reflux, 48 hours.

3.2 Optical and electronic properties

The UV-Vis absorption spectra of **MC124**, **MC125** and **MC127** in DMF solution are shown in **Figure 1** and related optical data are summarized in **Table 1**.

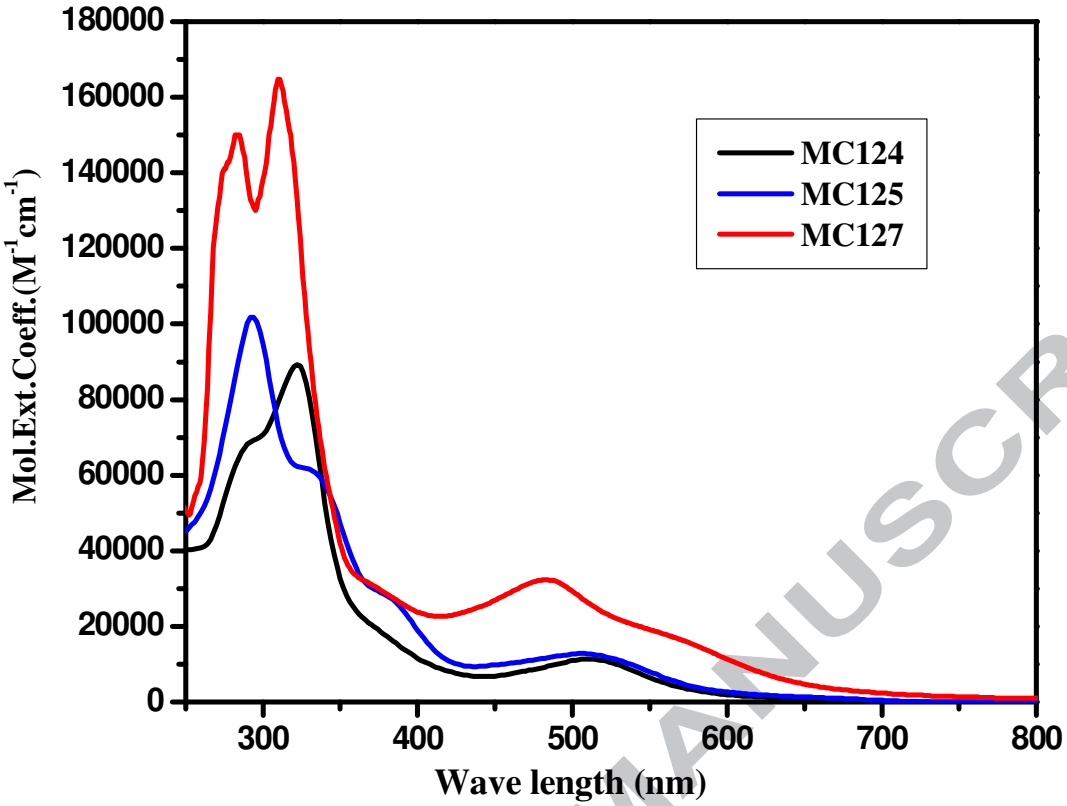

Figure.2: UV-vis absorption spectra of **MC124, MC125 and MC127** in DMF solution.

Table 1. Optical and electrochemical data of sensitizers **MC124**, **MC125** and **MC127**.

Dye	λ_{max}(ε×10^{4}M^{-1} m^{-1}) [nm][a]	E_{oxd}[mV][b]	$E_{0\text{-}0}$ [eV][c]	E^*_{oxd}[V][d]
MC124	511(1.137)	1.0919	2.218	-1.1261
MC125	505(1.289)	1.1268	2.167	-1.0402
MC127	483(3.249), 573(1.848)	1.1094	2.003	-0.8936

[a] absorption spectra were recorded in DMF, [b] oxidation potentials were measured by oxidative differential pulse voltammetry, [c] the bandgap $E_{0\text{-}0,}$ was derived from the intersection of absorption and emission spectra, [d] E^*_{oxd} were calculated by $E_{ox}{}^b$- $E_{o\text{-}o}{}^c$.

The **MC** dyes exhibit good optical properties with an intense absorption band in the range 250-400 nm and another band at longer wavelenghts in the range 430-600 nm. The absorption maxima follows the order **MC127**(483 nm) < **MC125**(505 nm) < **MC124**(511 nm) while the

molar extinction coefficient ($\mathcal{E}$) has an opposite trend (**MC124 < MC125 < MC127**). Overall, the thiocyanate free complex (**MC127**) shows the most promising optical properties, both in terms of wavelength and extinction coefficient while the fluorene and carbazole functionalized bipyridine dyes (**MC124** and **MC125**) show only slight differences from one another. As a reference, we compared the optical data of **MC** dyes with the optical properties of the black dye (**N749**). Concerning the absorption band in the visible range, a blue shift in the λ_{max} for all the three sensitizers compared to **N749** (620 nm) was observed, whereas the molar extinction coefficients are higher than **N749** ($0.8930*10^4 M^{-1}cm^{-1}$).[30]

Theoretical calculation has been performed in order to reproduce and rationalize the optical and electronic properties of **MC** sensitizers. For **MC124** and **MC125** complexes a good agreement between experimental and computed spectra has been observed as can be noted in **Table 2**, apart from a slight shift toward higher wavelengths (0.09-0.13 ev respectively). For the **MC127** bis-terpyridine complex we computed higher discrepancies between the experimental and theoretical spectra. It has to be noticed that we employed fully-deprotonated complex geometries in the simulation that is expected to provide blue shift absorption maxima.[62] In any case we were able to well reproduce the experimental trend in the wavelength of the absorption maxima.

Table 2. Comparison between experimental and computed λ_{max}.

Dye	**λ_{max} (Exp.)**		**λ_{max} (Theo.)**	
	nm	**eV**	**nm**	**eV**
MC124	512	2.42	494	2.51
MC125	506	2.45	480	2.58
MC127	483	2.57	433	2.86

In all the cases, the transitions in the visible region are assigned as MLCT while the band at lower wavelengths, in the range 250-400 nm, is due to the ligand centred π-π* electronic transition. The set of quasi degenerate HOMO-2/HOMO-1 and HOMO have essentially Ru t_{2g} character. For **MC124** and **MC125** the HOMOs are localized both on the Ru center and on the NCS ligand, **Figure 3**. The **MC127** present a higher band gap, due the significantly stabilized (0.5 eV) HOMO level, localized on the metal center, compared to **MC124** and **MC125**. Moving to the analysis of LUMOs, for **MC124** and **MC125** LUMO is localized on the bipyridine ligand while for the **MC127** it is localized on the terpyridine ligand, **Figure 3**. This result is in agreement with a previous publication by van Koten et al.[63] on similar terpyridine based Ru(II) dyes, and suggest an unfavorable localization of the electron density in the excited state. The calculated energy levels are in good agreement with the experimental data reported in **Table 1**.

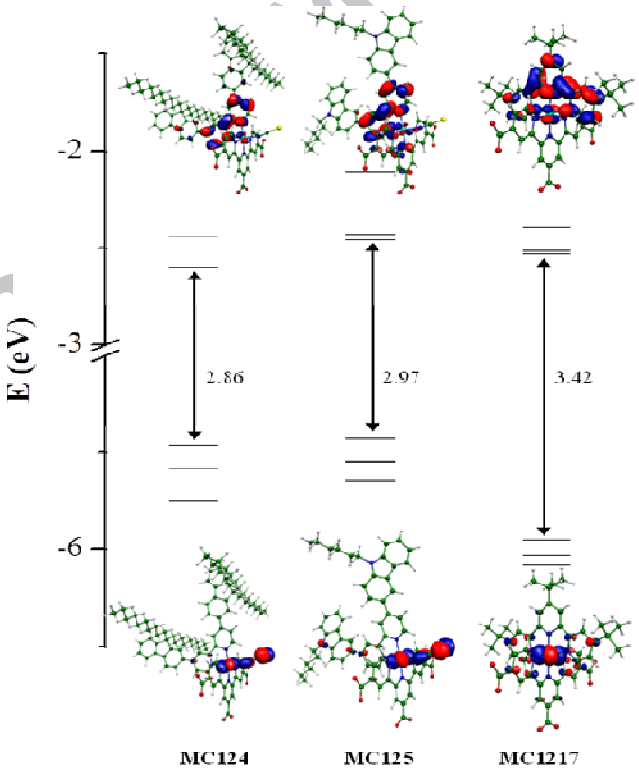

Figure 3. Schematic representation of the energy levels of the **MC124**, **MC125** and **MC127** complexes. Isodensity surface plots (isodensity contour: 0.035) of selected molecular orbitals are also shown.

The HOMO-LUMO levels are essential parameters to assess the ease of electron injection from the excited sensitizer to the conduction band (E_{cb}) of TiO_2 and the subsequent dye regeneration. Oxidative differential pulse voltammetry were performed with 0.1 tetrabutylammonium hexaflurophosphate as supporting electrolyte in DMF solution (**Figure 4**). All potentials were internally referenced to the ferrocene/ferrocenium (Fe/Fe^+) couple which has the redox potentials of ($E_{Fe/Fe+}$) 0.510 V vs Ag/AgCl. The first oxidation potentials of the dyes have been determined from their corresponding peak potentials and incorporated in the **Table 1**. The oxidation potentials of the $Ru^{III/II}$ are 1.0919, 1.1268 and 1.1094 V for **MC124**, **MC125** and **MC127**, respectively, **Figure 4** and **Table 1**. This potential is sufficiently more positive than I^-/I_3^- and provides enough driving force for effective dye regeneration. The excited-state oxidation potentials (E_{ox}^*) of **MC124**, **MC125** and **MC127** have been calculated from E_{oxd}-E_{0-0} formula,[64,65] are -1.1261, -1.0402 and -0.8936 V respectively, and are more negative than the conduction band edge of TiO_2 (-0.5 V) ensuring an efficient electron injection process from the excited state of the dyes into the TiO_2 electrode. The schematic energy level diagram for **MC124**, **MC125** and **MC127** has been shown in **Figure 4b** according to their electrochemical data.

a)

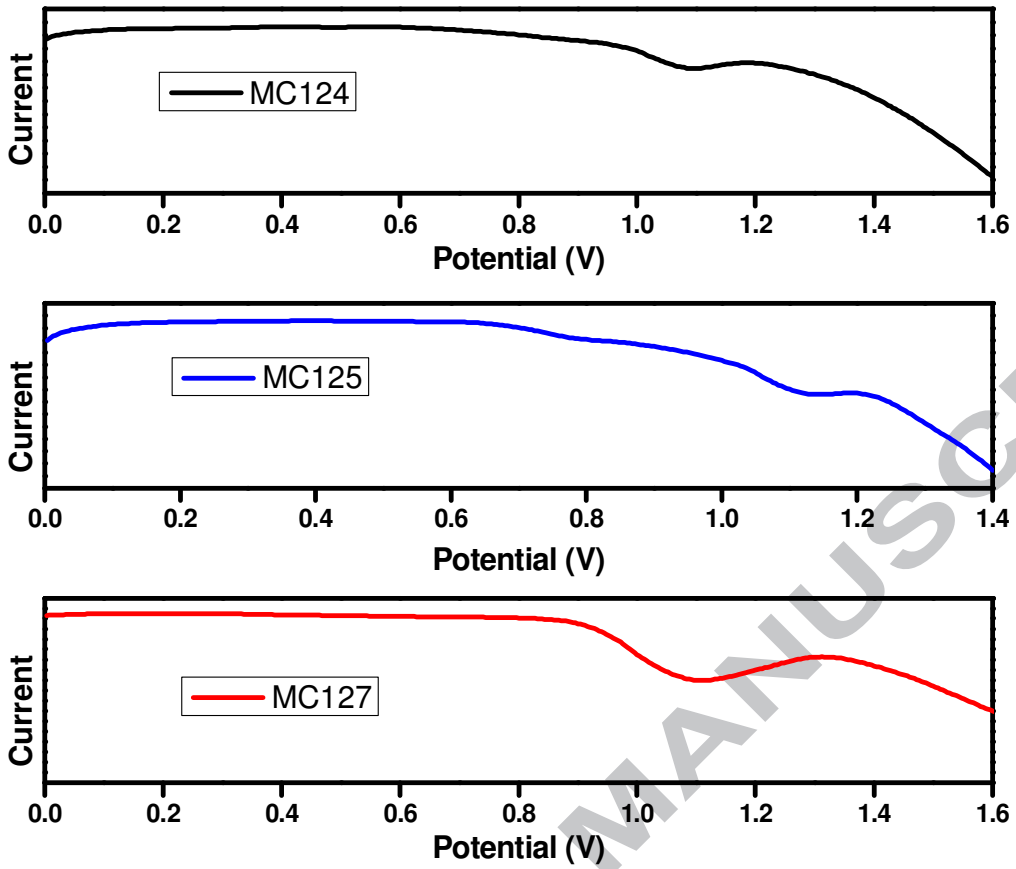

b)

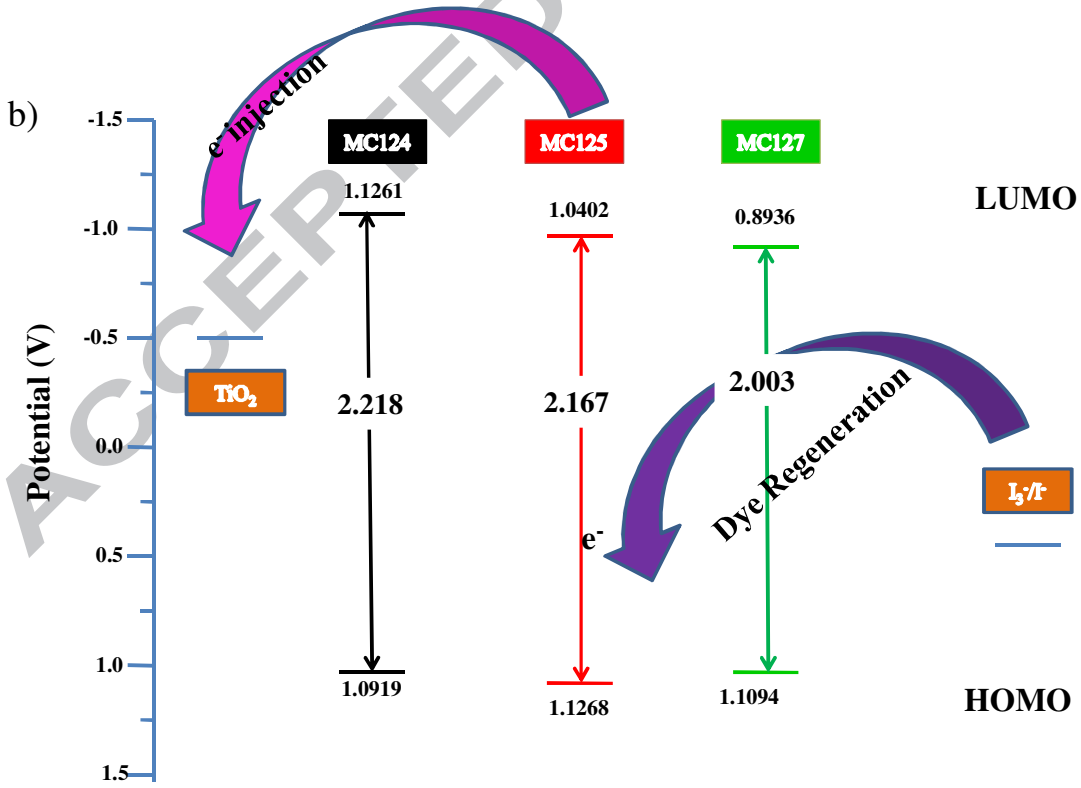

Figure 4. a) Oxidative differential pulse voltammetry of **MC124**, **MC125** and **MC127**. b) The schematic energy levels of **MC124**, **MC125** and **MC127** based on absorption and electrochemical data.

3. 3 Photovoltaic performances

After the optoelectronic characterization, several working devices have been realized with the aim to test the photovoltaic properties of **MC** ruthenium complexes. Details of devices fabrication are summarized in the experimental section. The J-V curves and the IPCE spectra are reported in **Figure 5** and the related photovoltaic data are summarized in **Table 3**.

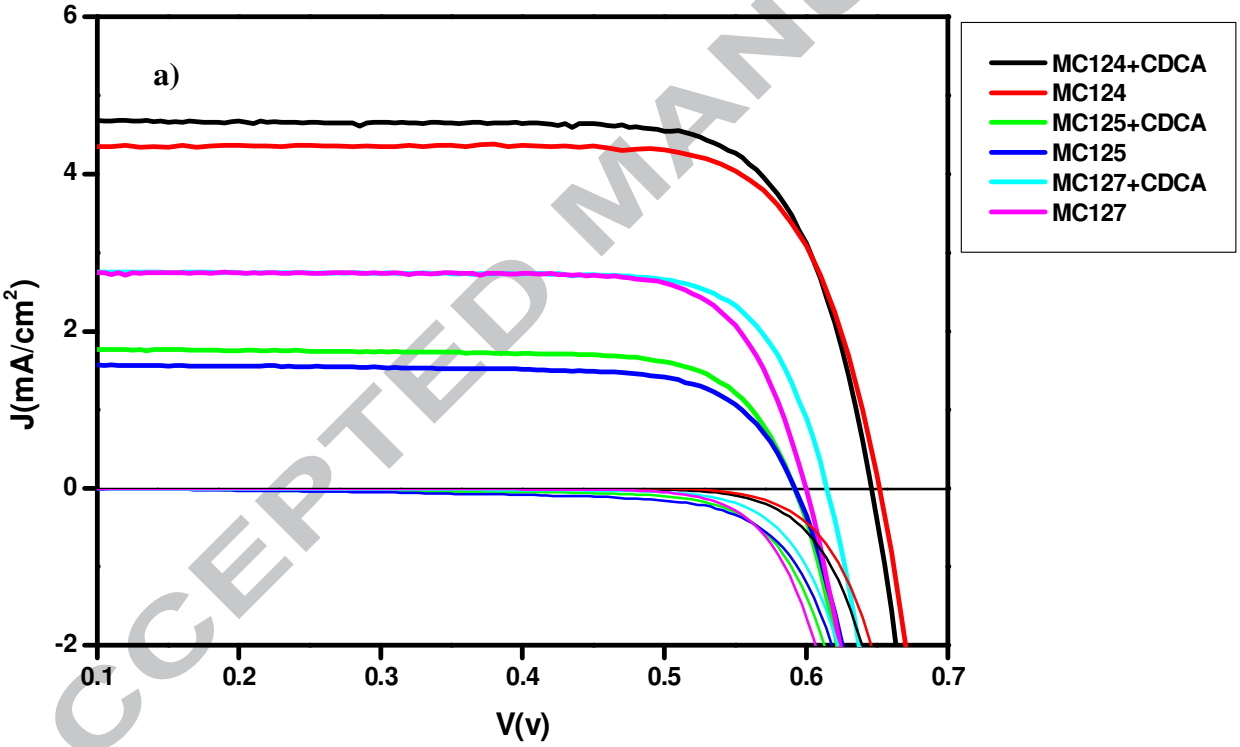

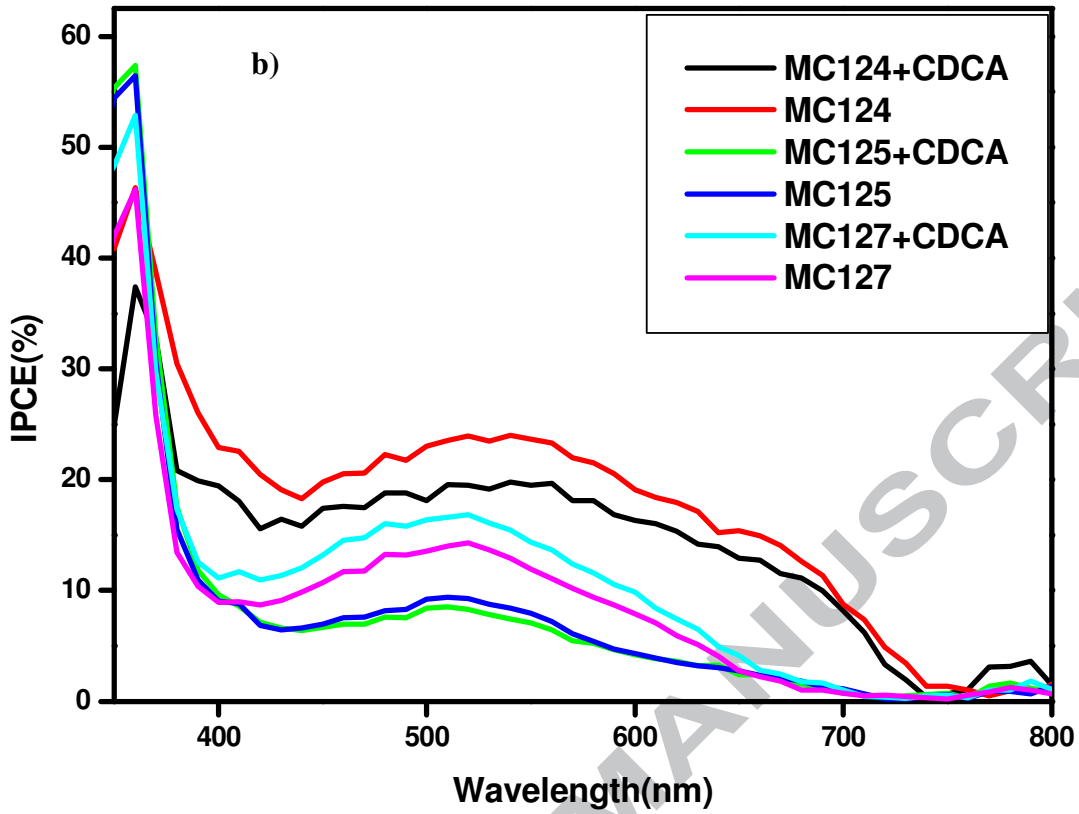

Figure 5. a) J-V curves and dark current b) IPCE spectra of the devices realized with **MC** dyes with and without CDCA added in the sensitization solutions.

Table 3. Photovoltaic data of working devices employing **MC** dyes and iodine based electrolyte. The average values of three devices are reported in parenthesis.

Dye	**CDCA**	**J_{sc}[a] (mA/cm^2)**	**V_{oc}[b] (mV)**	**FF[c]**	**η[d] (%)**
MC124	No	4.3(4.1)	641(647)	0.78(0.78)	2.1(2.1)
MC125	No	1.5(1.4)	590(592)	0.75(0.75)	0.7(0.7)
MC127	No	2.7(2.6)	594(596)	0.80(0.79)	1.3(1.2)
MC124	0.6 mM	4.6(4.4)	641(640)	0.78(0.78)	2.3(2.2)
MC125	0.6 mM	1.8(1.6	586(585)	0.76(0.75)	0.8(0.7)
MC127	0.6 mM	2.7(2.6)	609(605)	0.79(0.78)	1.3(1.2)

[a] Current density, [b] open-circuit voltage, [c] fill factor, [d] photoelectric conversion efficiency.

We started the test of all the **MC** dyes in standard conditions and, then we tried to improve the photovoltaic performances of the devices with the addition of the chenodeoxycholic acid co-adsorbent (CDCA) in the sensitizing solutions (**Table 3**). The addition of CDCA as co-adsorbent led only to a slight increase of Jsc and hence of the final efficiency, suggesting that the aggregation of dyes on the TiO_2 surface is not the major issue.

The best performances were obtained with **MC124** with a maximum PCE of 2.3%, due to the highest photocurrent density and photo voltage. The presence of long alkyl chains on the bipyridine ligand ensure a better packing onto TiO_2 surface probably leading to the reduction of parasitic recombination reactions.

Overall the photocurrent density has strongly limited the performances of devices employing **MC** dyes, **Table 3**. The low photocurrent densities are probably due to electron injection problems caused by an unfavorable localization of the electron density in the excited state, that is far from the carboxylic anchoring group (**Figure 3**). A similar behavior has been observed for other terpyridine-based ruthenium dyes which have shown low IPCE values.[63] Another possible explanation for the low performances of **MC** dyes, could be the parasitic recombination reactions competing with the regeneration of dye molecules. Clifford et al.[66] in 2007 have shown that the regeneration process of ruthenium dyes proceed via the formation of an intermediate species between Ru(II) oxidized dye and iodide ions in the electrolyte. The most likely mechanism for the interaction between oxidized dyes and iodide is the binding of iodide to the S atom of the thiocyanate groups[67] as confirmed by theoretical calculations.[68] Thus the partial (**MC124** and **MC125**) or total (**MC127**) replacement of thiocyanate could make the regeneration of oxidized dye molecules difficoult. It has to be noted, furthermore, that for the oxidized **MC127** dye, the

hole remains confined on the ruthenium metal, where the HOMO orbital is localized. The terpyridine ligand bearing the bulky tert-butyl substituents thus could inhibit the regeneration process keeping the redox mediator far from the dye hole.

Concerning the stability, direct long-term stability test have not been performed. However similar terpyridine-based dyes have shown very good photostability upon prolonged irradiation in both Ru(II) and oxidized Ru(III) state[63] Moreover the presence of three carboxylic anchoring groups suggests a strong adsorption onto the titania surface, as already reported in our previous papers.[48]

4. Conclusions

Summarizing we have reported the design and synthesis of three novel Ru(II) complexes, **MC** dyes. The **MC** dyes employ 2,2':6',2''-terpyridine-4,4',4''-tricarboxylic acid as anchor group, and alternatively a bipyridine (**MC124** and **MC125**) and terpyidine (**MC127**) auxiliary ligands, partially or totally replacing the thiocyanate groups of the reference **N749** dye. The dyes were initially characterized from the optoelectronic side, employing ~~cyclic voltammetry~~ DPV and recording the UV-vis absorption spectra in solution. All the **MC** dyes exhibit good optical properties, with an absorption band in the visible range (430-600 nm) characterized by molar extinction coefficients higher than the reference **N749** dye. The **MC** dyes also shown good electronic properties with an adequate positioning of energy levels. The ground state oxidation potentials are more positive than the I^-/I^-_3 redox couple which should provide enough driving force for the effective dye regeneration, and the excited state oxidation potentials values are more negative than the conduction band edge of TiO_2 ensuring an efficient electron injection process. After the optoelectronic characterization, the **MC** dyes were tested in working devices with iodine based electrolyte. The overall performances were quite low, mainly due to the poor generated photocurrent that has been possibly related to an unfavorable LUMO localization far from the anchoring sites. Further improvements could be achieved by modification of molecular structure.

Acknowledgements:

GK thanks CSIR, New Delhi and P.CH thanks UGC, for senior research fellowships. MC thanks DST, New Delhi for funding the project No. DST/TMC/SERI/FR/92

References:

1. B. O'Regan, M. Grätzel, Nature 353 (1991) 737.
2. T. M. Brown, F. De Rossi, F. Di Giacomo, G. Mincuzzi, V. Zardetto, A. Realea A. Di Carloa, J. Mater. Chem. A, 2 (2014) 10788.
3. N. G. Park, J. van de Lagemaat and A. J. Frank, J. Phys. Chem. B, 104 (2000) 8989.
4. D. Kuang, S. Ito, Wenger, C. B. Klein, J. E. Moser, R. Humphry-Baker, S. M. Zakeeruddin, M. Grätzel, J. Am. Chem. Soc. 128 (2006) 4146.
5. D. Kuang, C. Klein, S. Ito, J. E. Moser, R. Humphry-Baker, S. M. Zakeeruddin, M. Grätzel, Adv. Funct. Mater. 17 (2007) 154.
6. D. Kuang, C. Klein, S. Ito, J. E. Moser, R. Humphry-Baker, N. Evans, F. Duriaux, C. Grätzel, S. M. Zakeeruddin, M. Grätzel, Adv. Mater. 19 (2007) 1133.
7. J.-W. Shiu, Z.-J. Lan, C.-Y. Chan, H.-P. Wu and E. W.-G. Diau, J. Mater. Chem. A, 2, (2014) 8749.
8. S. S. Mali, H. Kim, C. S. Shim, P. S. Patil, J. H. Kim and C. K. Hong, Sci. Rep. 3 (2013) 3004.
9. Y. Ooyama and Y. Harima, Eur. J. Org. Chem. (2009) 2903.
10. Y.-S. Yen, H.-H. Chou, Y.-C. Chen, C.-Y. Hsu and J. T. Lin, J. Mater. Chem. 22 (2012) 8734.
11. M. Zhang, Y. Wang, M. Xu, W. Ma, R. Li and P. Wang, Energy Environ. Sci. 6 (2013) 2944.
12. M. Liang and J. Chen, Chem. Soc. Rev. 42 (2013) 3453.
13. Y. Wu and W. Zhu, Chem. Soc. Rev. 42 (2013) 2039.
14. A. Yella, C.-L. Mai, S. M. Zakeeruddin, S.-N. Chang, C.-H. Hsieh, C.-Y. Yeh and M. Grätzel, Angew. Chem., Int. Ed., 53 (2014) 2973.
15. C.-L. Wang, J.-Y. Hu, C.-H. Wu, H.-H. Kuo, Y.-C. Chang, Z.-J. Lan, H.-P. Wu, E. Wei-GuangDiau and C.-Y. Lin, Energy Environ. Sci. 7 (2014) 1392.
16. S. Mathew, A. Yella, P. Gao, R. Humphry-Baker, F. E. CurchodBasile, N. Ashari-Astani, I. Tavernelli, U. Rothlisberger, M. K. Nazeeruddin and M. Grätzel, Nat. Chem. 6 (2014) 242.

17. P. Xie and F. Guo, Curr. Org. Chem. 15 (2011) 3849.
18. P. G. Bomben, K. C. D. Robson, B. D. Koivisto and C. P. Berlinguette, Coord. Chem. Rev., 2012, 256, 1438.
19. J.-F. Yin, M. Velayudham, D. Bhattacharya, H.-C. Lin and K.-L. Lu, Coord. Chem. Rev., 256 (2012) 3008.
20. S. Miura, H. Uchida, S. Takata, M. Sumioka, K. Liska, P. Comte, P. Pechy, P. Gratzel, M. Chem. Commun. (2008) 5194.
21. Zeng, W.; Cao, Y.; Bai, Y.; Wang, Y.; Shi, Y.; Zhang, M.; Wang, F.; Pan, C.; Wang, P. Chem. Mater. 22 (2010) 1915.
22. A. Yella, C.-L. Mai, S. M. Zakeeruddin, S.-N. Chang, C.-H. Hsieh, C.-Y. Yeh and M. Gr¨atzel, Angew. Chem., Int. Ed. 53 (2014) 2973.
23. C.-L. Wang, J.-Y. Hu, C.-H. Wu, H.-H. Kuo, Y.-C. Chang, Z.-J. Lan, H.-P. Wu, E. Wei-GuangDiau and C.-Y. Lin, Energy Environ. Sci. 7 (2014) 1392.
24. S. Mathew, A. Yella, P. Gao, R. Humphry-Baker, F. E. CurchodBasile, N. Ashari-Astani, I. Tavernelli, U. Rothlisberger, M. K. Nazeeruddin and M. Gr¨atzel, Nat. Chem. 6 (2014) 242.
25. H. Heo, S. H. Im, J. H. Noh, T. N. Mandal, C.-S. Lim, J. A. Chang, Y. H. Lee, H.-J. Kim, A. Sarkar, M. K. Nazeeruddin, M. Grätzel, S. I. Seok, Nat. Photonics, 7 (2013) 486.
26. M. A. Green, A. Ho-Baillie and H. J. Snaith, Nat. Photon. 8 (2014) 506.
27. H. Zhou, Q. Chen, G. Li, S. Luo, T.-b. Song, H.-S. Duan, Z. Hong, J. You, Y. Liu and Y. Yang, Science, 345, (2014) 542.
28. M. K. Nazeeruddin, P. Pechy, T. Renouard, S. M. Zakeeruddin, R. Humphry-Baker, P. Comte, P. Liska, L. Cevey, E. Costa, V. Shklover, L. Spiccia, G. B. Deacon, C. A. Bignozzi, M. Grätzel, J. Am. Chem. Soc. 123 (2001) 1613.
29. T. Funaki, M. Yanagida, N. Onozawa-Komatsuzaki, K. Kasuga, Y. Kawanishi, M. Kurashige, K. Sayama, H. Sugihara, Inorganic Chemistry Communications 12 (2009) 842.
30. K. Ganesh, B. Vinayak, T. Suresh, W. Guohua, L. Jingzhe, F. Xiaqin, K. Fantai, D. Songyuan, S. Niveditha, K. Bhanuprakash, M. Chandrasekharam, Dalton Trans. 43 (2014) 14992.
31. S.-H. Yang, K.-L. Wu, Y. Chi, Yi-M. Cheng, Pi-T. Chou, Angew. Chem., Int. Ed. 50 (2011) 8270

32. K.-L. Wu, C.-H. Li, Y. Chi, J. N. Clifford, L. Cabau, E. Palomares, Yi-M. Cheng, H.-A. Pan and Pi-T. Chou, J. Am. Chem. Soc. 134 (2012) 7488.
33. Y. Numata, S. P. Singh, A. Islam, M. Iwamura, A. Imai, K. Nozaki and L. Han, Adv. Funct. Mater., 23 (2013) 1817.
34. W. Kubo, A. Sakamoto, T. Kitamura, Y. Wada, S. Yanagida, J. Photochem. Photobiol. A, 164 (2004) 33.
35. M. Dürr, A. Bamedi, A. Yasuda, G. Nelles, Appl. Phys. Lett. 84 (2004) 3397.
36. M. Murayama, T. Mori, J. Phys. D, 40 (2007) 1664.
37. K. Sayama, S. Tsukagoshi, T. Mori, K. Hara, Y. Ohga, A. Shinpou, Y. Abe, S. Suga, H. Arakawa, Sol. Energ. Mater. Sol. Cells 80 (2003) 47.
38. J.N. Clifford, E. Palomares, M.K. Nazeeruddin, R. Thampi, M. Grätzel, J.R. Durrant, J. Am. Chem. Soc. 126 (2004) 5670.
39. V.P.S. Perera, P.K.D.D.P. Pitigala, M.K.I. Senevirathne, K. Tennakone, Sol. Energ. Mater. Sol. Cells 85 (2005) 91.
40. Y. Chen, Z. Zeng, C. Li, W. Wang, X. Wang, B. Zhang, New J. Chem. 29 (2005) 773.
41. J.-H. Yum, S.-R. Jang, P. Walter, T. Geiger, F. Nüesch, S. Kim, J. Ko, M. Grätzel, M.K. Nazeeruddin, Chem. Commun. (2007) 4680.
42. F. Inakazu, Y. Noma, Y. Ogomi, S. Hayase, Appl. Phys. Lett. 93 (2008) 093304.
43. P. Salvatori, S. Agrawal, C. Barreddi, C. Malapaka, M. D. Borniol, F. D. Angelis, RSC. Advances 4 (2014) 57620.
44. S.-W. Wang, C.-C. Chou, F.-C. Hu, K.-L. Wu, Y. Chi, J. N. Clifford, E. Palomares, S.-H. Liu, P.-T. Chou, T.-C. Wei, T-Y. Hsiao J. Mater. Chem. A, 2 (2014) 17618.
45. A. R. Andersen, J. Halme, T. Lund, M. I. Asghar, P. T. Nguyen, K. Miettunen, E. Kemppainen O. Albrektsen, J. Phys. Chem. C, 115 (2011) 15598.
46. H. T. Nguyen, H. M. Ta and T. Lund, Sol. Energy Mater. Sol. Cells, 91 (2007) 1934.
47. P. T. Nguyen, R. Degn, H. T. Nguyen and T. Lund, Sol. Energy Mater. Sol. Cells, 93 (2009) 1939.
48. M. G. Lobello, K-L. Wu, M. A. Reddy, G. Marotta, M. Grätzel, M. K. Nazeeruddin, Y. Chi, M. Chandrasekharam, G. Vitillaro, F. D. Angelis. Dalton Trans. 43 (2014) 2726.

49. L. Han, A. Islam, H. Chen, M. Chandrrasekharam, B. Chiranjeevi, S. Zhang, X. Yang, M. Yanagida, Energy Environ. Sci. 5 (2012) 6057.
50. M. Chandrasekharam, M. A. Reddy, S. P. Singh, B. Priyanka, K. Bhanuprakash, M. Lakshmi Kantam, A. Islam L. Han.J. Mater. Chem., 22 (2012) 18757.
51. M. Chandrasekharam, T. Suresh, S. P. Singh, B. Priyanka, K. Bhanuprakash, A. Islam, L. Han, M. Lakshmi Kantama. Dalton Trans. 41 (2012) 8770.
52. T. Suresh, G. Rajkumar, S. P. Singh, P. Y. Reddy, A. Islam, L. Han, M. Chandrasekharam, Org. Electron. 14 (2013) 2243.
53. T. Suresh, K. Ganesh, S. P. Singh, A. Islam, L. Han, M. Chandrasekharama, Dyes and Pigments 99, (2013) 850.
54. M. Chandrasekharam, G. Rajkumar, Ch. SrinivasaRao, T. Suresh, P. Y. Reddy, J-H. Yum, M. K. Nazeeruddin, M. Grätzel, Nanosci. Nanotechnol., 2 (2011) 1.
55. G.; Marotta, , Ch. P. Kumar, M. G. Lobello, Cavazzini, F.; Salvatori, P.; Ganesh, K.; Nazeeruddin, M. K.; Chandrasekharam, M.; De Angelis, F. Dalton Trans. 44 (2015) 5369.
56. M. J. Frisch, G. W. Trucks, H. B. Schlegel, G. E. Scuseria, M. A. Robb, J. R. Cheeseman, J. A. J. Montgomery, T. Vreven, K. N. Kudin, J. C. Burant, J. M. Millam, S. S. Iyengar, J. Tomasi, V. Barone, B. Mennucci, M. Cossi, G. Scalmani, N. Rega, G. A. Petersson, H. Nakatsuji, M. Hada, M. Ehara, K. Toyota, R. Fukuda, J. Hasegawa, M. Ishida, T. Nakajima, Y. Honda, O. Kitao, H. Nakai, M. Klene, X. Li, J. E. Knox, H. P. Hratchian, J. B. Cross, V. Bakken, C. Adamo, J. Jaramillo, R. Gomperts, R. E. Stratmann, O. Yazyev, A. J. Austin, R. Cammi, C. Pomelli, J. W. Ochterski, P. Y. Ayala, K. Morokuma, G. A. Voth, P. Salvador, J. J. Dannenberg, V. G. Zakrzewski, S. Dapprich, A. D. Daniels, M. C. Strain, O. Farkas, D. K. Malick, A. D. Rabuck, K. Raghavachari, J. B. Foresman, J. V. Ortiz, Q. Cui, A. G. Baboul, S. Clifford, J. Cioslowski, B. B. Stefanov, G. Liu, A. Liashenko, P. Piskorz, I. Komaromi, R. L. Martin, D. J. Fox, T. Keith, M. A. Al-Laham, C. Y. Peng, A. Nanayakkara, M. Challacombe, P. M. W. Gill, B. Johnson, W. Chen, M. W. Wong, C. Gonzalez and J. A. Pople, 2009
57. A. D. Becke, J. Chem. Phys., 98 (1993) 5648.
58. J. S. Binkley, J. A. Pople and W. J. Hehre, J. Am. Chem. Soc. 102 (1980) 939.
59. N. Godbout, D. R. Salahub, J. Andzelm and E. Wimmer, Can. J. Chem., 70 (1992) 560.
60. M. Cossi and V. Barone, J. Chem. Phys. 115 (2001) 4708.

61. S. Miertuš, E. Scrocco and J. Tomasi, Chem. Phys. 55(1981), 117

62. S. Fantacci, M.G. Lobello, F. De Angelis, Chimia 67 (2013) 121.

63. S.H. Wadman, J.M. Kroon, K. Bakker, R.W.A. Havenith, G.P.M. van Klink, G. van Koten, Organometallics 29 (2010) 1569.

64. A. Venkateswararao, K. R. Justin Thomas, C.-P. Lee, C.-T. Li, K.-C. Ho, ACS Appl. Mater. Interfaces, 6 (2014)2528.

65. K. R. Justin Thomas, N. Kapoor, C.-P. Lee, and K.-C. Ho, Chem. Asian J. 7 (2012) 738.)

66. J. N. Clifford, E. Palomares, M. K. Nazeeruddin, M. Grätzel, J. R. Durrant, J. Phys. Chem. C. 111 (2007) 6561.

67. T. Privalov, G. Boschloo, A. Hagfeldt, P. H. Svensson, L. J. Kloo, Phys. Chem. C 113 (2009) 783.

68. M. G. Lobello, S. Fantacci, F. De Angelis, J. Phys. Chem. C 115 (2011) 18863.

New Terpyridine-based Ruthenium Complexes for Dye Sensitized Solar Cells Applications

Ganesh Koyyada,[a,b] Pavan Kumar CH, [a,b] Paolo Salvatori,[c,d] Gabriele Marotta,[c,e] Maria Grazia Lobello,[c] Olivia Bizzarri,[c] Filippo De Angelis,*[c] Chandrasekharam Malapaka*[a,b]

Three new Terpyridine based Ruthenium sensitizers coded as **MC124**, **MC125** and **MC127** have been synthesised and evaluated for DSSC. All the dyes showed high molar extinction coefficients than that of standard N749.

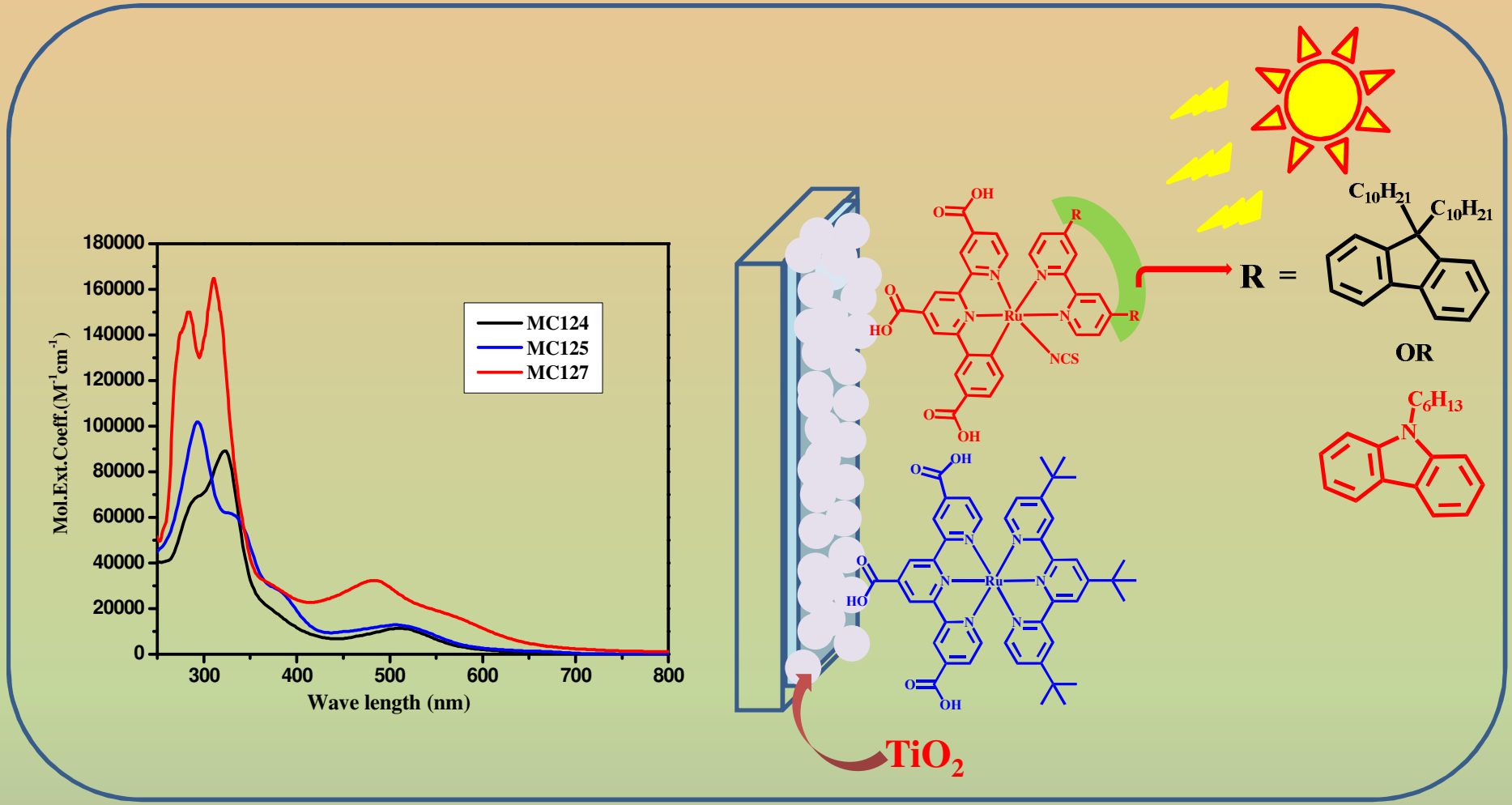

Synopsis

Here we report three new ruthenium terpyridine complexes with and without thiocyanate for the application in dye sensitized solar cells. Here the terpyridinic acid ligand acts as an anchoring group. Sensitizer **MC124** found to be more efficient compared to **MC125** and **MC127**.

Highlights

- We have successfully designed and synthesized three new terpyridine based Ruthenium Complexes with single thiocyante (MC124, MC125) and thiocyante free (**MC127**).
- All three sensitizers showed higher molar extinction coefficients compared to **N749**.
- We have evaluated these sensitizers for DSSCs with CDCA and Without CDCA
- **MC124** exhibited high power conversion efficiency of 2.3%.
- The experimental parameters are in good agreement with theoretically computed values.